# 3. INTRODUCTION

This is the final report for Clean Air Research Project 11 “A methodology for determining the impact of climate change on ozone levels in an urban area” which was funded by the Department of Environment, Water Resources, Heritage and the Arts (DEWHA) and undertaken by CSIRO Marine and Atmospheric Research (CMAR) with the support of NSW Department of Environment and Climate Change (DECC). The primary objective of this project was to demonstrate a methodology that is able to give estimates of ozone concentrations under climate change conditions for any period or location in Australia, and to specifically give an insight into the impact of climate change on ozone levels in Sydney in 20 and 50 years time. A second objective was to estimate the decrease of emissions which may be needed to maintain ozone levels below the Ambient Air Quality National Environment Protection Measure (AAQ NEPM) standards established by the National Environment Protection Council (NEPC). The tools that were developed and assessed in this project are intended to provide a capability that can aid policy makers in formulating long term air pollution policies where the impact of climate change needs to be considered.

## 3.1 Purpose

The purpose of this report is to document the work completed for Clean Air Research Project 11 and includes the following.

1. A description of the system which we have developed to downscale coarse resolution Global Climate System Model (GCM) climatology’s to urban scale resolution; and to model the photochemical transformation of ozone precursors at regional and urban scales.

2. An introduction to the methodologies used for modelling temperature dependent anthropogenic and natural emissions.

3. A review of the performance of the Cubic Conformal Atmospheric Model (CCAM; McGregor and Dix 2005) in downscaling a GCM global climatology to 60 km grid spacing over Australia.

4. A review of the performance of TAPM (Hurley 2005) in downscaling the CCAM meteorological fields to 3 km grid spacing over Sydney.

5. A review of the performance of TAPM–CTM (Chemical Transport Model; Cope et al. 2005) in modelling peak ozone concentrations in the Sydney Greater Metropolitan Region (GMR).

6. An introduction to the use of synoptic typing to verify the ozone climatology generated by the downscaling system.

7. An overview of indicative changes in peak ozone concentrations (and related health impacts) in 2021–2030 and 2051–2060 due to the modelled climate change scenario.
8. An analysis of the factors leading to changes in peak ozone for the modelled climate change scenario.
9. An overview of indicative changes in peak ozone concentrations in 2021–2030 and 2051–2060 due to both climate change and to changes in the anthropogenic precursor inventory and a consideration of the level of reduction of anthropogenic precursor emissions required for peak ozone in Sydney to comply with designated ozone standards in 2051–2060.
10. A discussion of the project ramifications, limitations and areas of future development.

## 3.2 Background

Photochemical smog in Australian cities has the greatest impact during the summer months when ambient temperatures and solar radiation fluxes are high and temperature dependent emission rates of volatile organic compounds (VOCs) from anthropogenic and vegetation sources are at their peak. With the majority of the Australian capital cities located on the coast, photochemical smog episodes are often associated with sea breeze conditions, with smog precursors, including oxides of nitrogen ($NO_x$), carbon monoxide (CO) and VOCs being transported offshore by land breezes and then recirculated inland by the action of the sea breeze. Elevated concentrations of ozone (the principal component of photochemical smog in Australia) may also be associated with bushfires and controlled burns, with ozone generation from VOCs, $NO_x$ and CO released by fires contributing to the photochemical smog generated from urban precursor plumes.

The severity of photochemical smog in Australian cities may be investigated through comparison of air quality network observations of ozone with the Ambient Air Quality National Environment Projection Measure (AAQ NEPM) ozone standards of 100 ppb (1–hour average) and 80 ppb (4–hour average) for ozone. This is illustrated in Figure 1 which shows that the AAQ NEPM standards for ozone were exceeded on occasions at all of the displayed capital cities over 1991–2001, with Sydney being of particular concern. More recent data indicates that there is little change in the exceedence statistics for this region (DECC 2006).

The relationship between climate change and air quality is an area which is under active investigation (i.e. see the review of Jacob and Winner 2008; also see Walsh 2008 for a review with emphasis on the Australian environment). Ozone is of particular concern because elevated ambient temperatures lead to increased ozone generation. Global scale modelling using global climate models (GCMs) coupled to global chemical transport models (GCTMs) suggest a non-linear response of the global troposphere ozone background concentrations to global warming. In regions remote from pollution, it is possible that background ozone concentrations may be reduced in the lower troposphere, as higher water vapour concentrations lead to ozone destruction under conditions of low $NO_x$ concentrations (Wu et al. 2008b). For polluted regions, modelling studies suggest that background ozone concentrations may increase by 1–10 ppb (Jacob and Winner 2008).

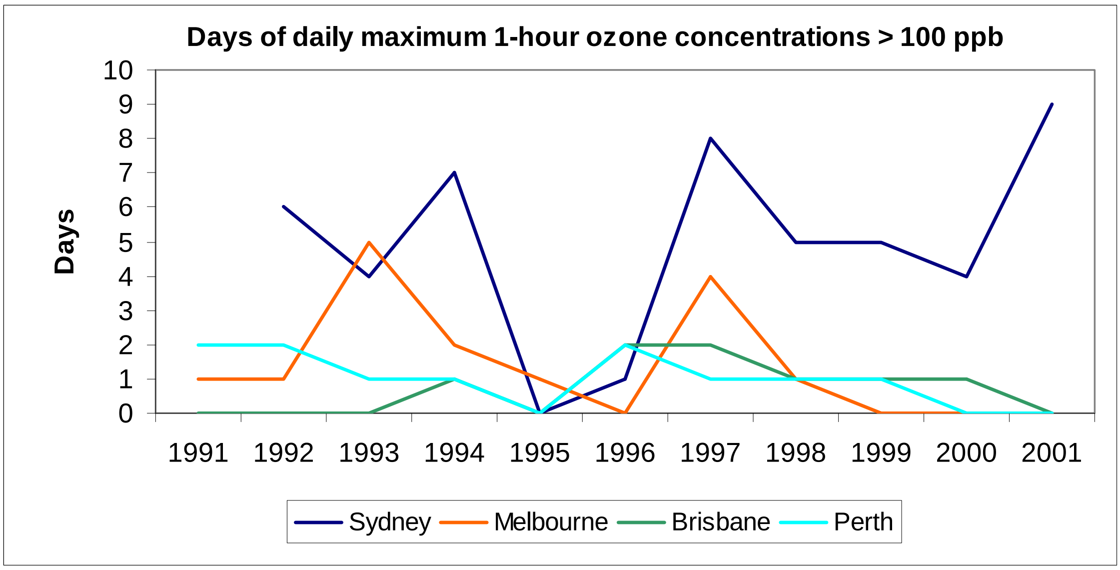

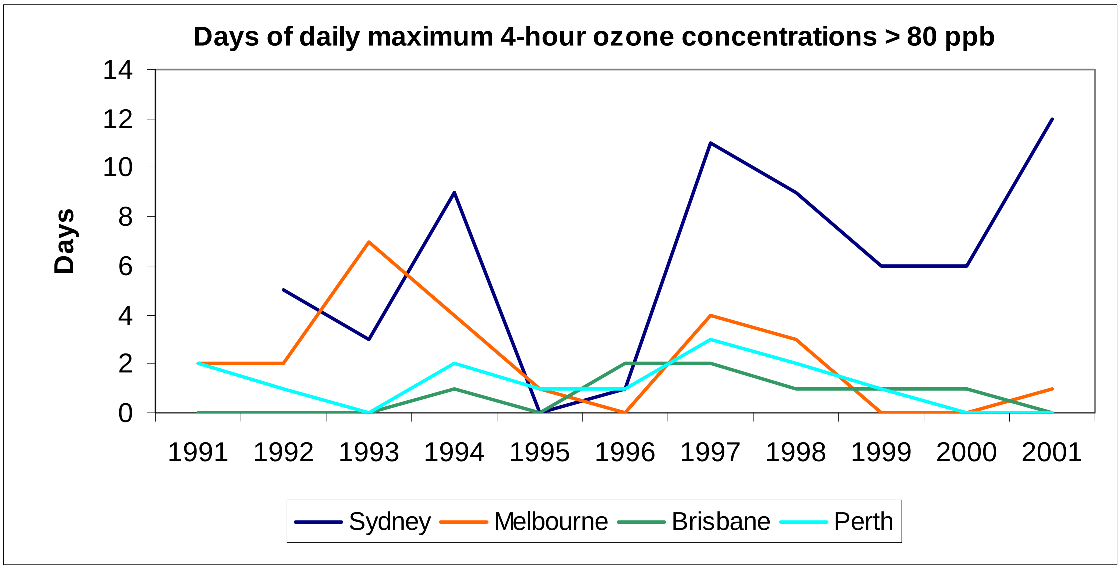

Figure 1 Number of days per year that the (top) 1–hour and (bottom) 4–hour ozone standards are exceeded at one or more monitoring stations in four of Australia's capital cities (SOE2006)

Researchers have recently been using the method of dynamical downscaling to investigate regional changes in ozone (e.g. Bell et al., 2007; Dawson et al. 2008; Hogrefe et al., 2004; Huang et al. 2008; Nolte et al. 2008; Meleux et al. 2007; Tagaris et al. 2007; Zhang et al. 2008). Dynamical downscaling consists of nesting a regional scale numerical weather prediction system (NWPS) within a coarser resolution GCM (typically 200 km grid spacing) and generating high resolution meteorological fields (typically 10–30 km) over a regional area. These meteorological fields and an air emissions inventory are then used by a chemical transport model (CTM) to simulate air pollution formation, transport and loss. Species concentrations at the boundaries of the CTM may be generated from the output of a GCTM, thereby enabling the impact of changes in the global background pollutant loadings under climate changes to also be included in the regional scale air pollutant fields.

The main task of the project documented in this report was to develop a dynamical downscaling system for investigating the response of urban ozone in Australian cities to climate change. The system was tested in Sydney, which was selected on the basis of having the highest frequency of ozone exceedences in Australia (Figure 1). The global climate simulations were based on an A2 Special Report on Emissions Scenario (A2 SRES) while the local anthropogenic emissions for Sydney were initially fixed to a current business-as-usual scenario in order to isolate the impact of climate change alone (the ‘Climate Penalty’). Following this first round of simulations, the system was re-run for 2051–2060 with the anthropogenic inventory modified to reflect population and energy increases and the development of more energy- and emissions-efficient technology that are consistent with the assumptions of the A2 SRES family of emission scenarios. A suite of worst case events were then selected from the 2051–2060 simulations and run with base inventory emissions of $NO_x$, VOCs and CO scaled by various factors in order to estimate the emission reduction required to achieve compliance with the AAQ NEPM goals for ozone.

Ten year periods were chosen for detailed high-resolution chemical transport simulations (1996-2005 [decade 1], 2021–2030 [decade 2] and 2051–2060 [decade 3]) in order to enable the inter-annual variability in ozone climate to be addressed. Even so, it must be stressed that the results presented in this report for 2021–2030 and 2051–2060 are based on a single climate change projection. The state-of-science in the area of climate change projection is based on the interpretation of an ensemble of GCM simulations (encompassing the use of different GCMs and emission scenarios), generally with the use of statistical downscaling methodologies for generating regional scale probabilistic projections (CSIRO 2007). As such, it should be emphasised that the primary purpose of the current project is to investigate the ability of the system to realistically downscale GCM climatology’s to urban scales. The results that we then present for ozone in 2021–2030 and 2051–2060 are intended to demonstrate the types of output that the system will be able to provide to regulators for policy development.

# 4. DESCRIPTION OF THE MODELLING SYSTEM

The downscaling system set up for this project is shown schematically in Figure 2 and consists of nesting TAPM–CTM, an urban/regional atmospheric transport and chemistry model (3-km inner grid spacing; Hurley 2005; Cope et al. 2004), into the regional meteorological fields (60-km grid spacing) generated by the stretched grid atmospheric model CCAM (McGregor and Dix 2005) which in turn is nudged towards global-scale meteorological fields generated by the CSIRO–Mk3 Global Climate System Model (Gordon et al. 2002). As noted in the previous section, CSIRO–Mk3 and CCAM were forced by one of a family of A2 Special Report on Emissions Scenarios (SRES).

Note that the chemical transformation modelling is undertaken only on the TAPM–CTM grids (the CGCM and CCAM do not currently treat detailed chemical transformation) and thus there is no transfer of changes in trace gas species concentrations into the TAPM–CTM domain, as a result of changes in global background concentrations.

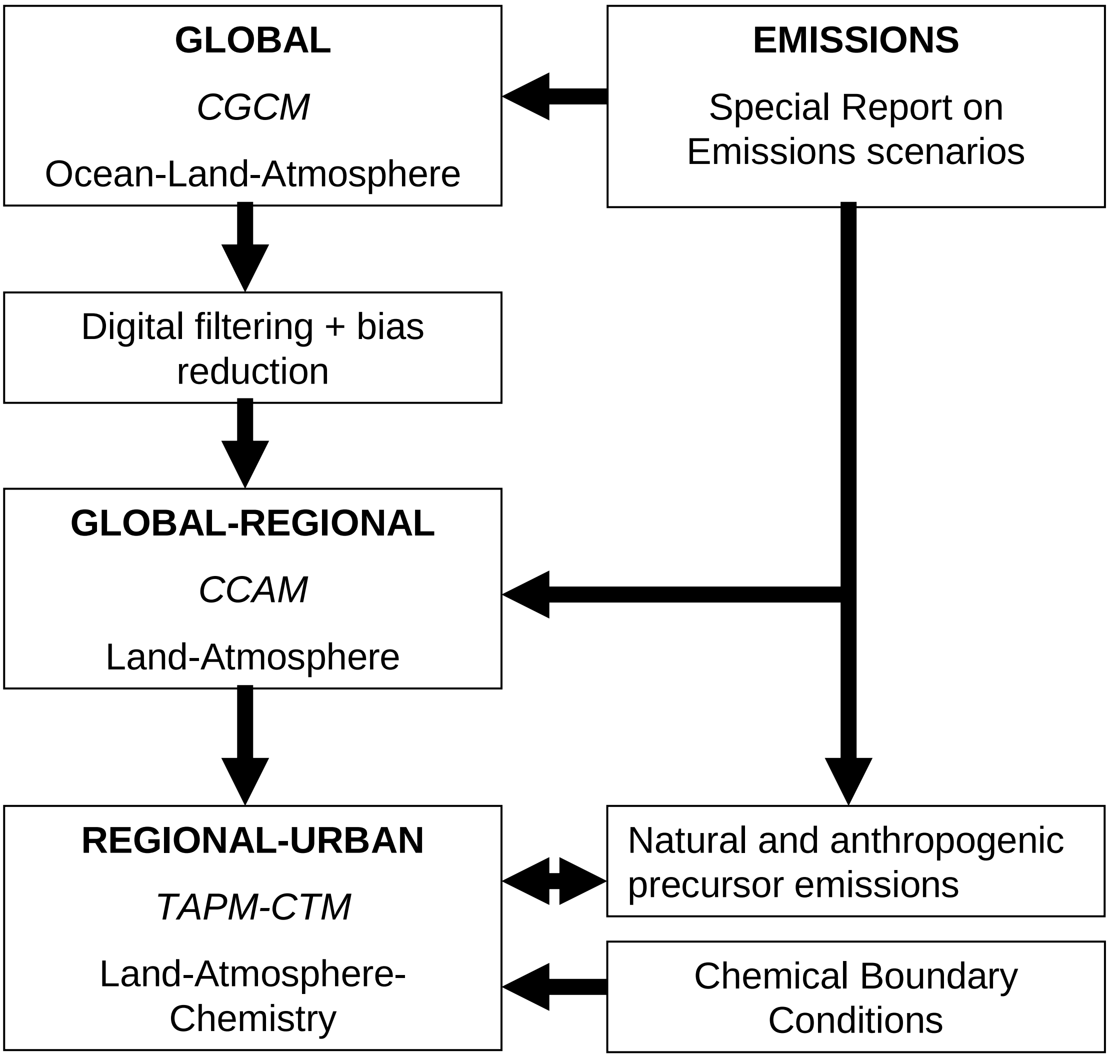

Figure 2. Schematic diagram showing the components of the dynamic downscaling system. See the text for a description of the individual components of the system.

As such the chemical boundary conditions for outer CTM grid are held fixed (at current observed continental and rural background concentrations) for all of the climate change air quality simulations. Thus the simulations were not able to take into account variations in the concentrations of ozone and precursor gases as a result of climate change or projected changes in global emissions. This assumption is considered in more detail in Section 8.3.

## 4.1 CSIRO–Mk3

The CSIRO–Mk3 Climate System model (CGCM; Gordon et al. 2002) has been extensively used by CSIRO for the development of climate change scenarios in response to the requirements of the IPCC. The model includes a comprehensive representation of the four major components of the climate system- atmosphere, land surface, oceans and sea ice. The atmospheric component uses a T63 spectral grid (1.875° EW x 1.875° NS- approximately 150–200 km grid spacing in the horizontal) with 18 vertical levels with the lowest level being

165 m above ground level and the top of the model domain extending to 36355 m above the ground. A feature at the atmospheric model is a detailed prognostic cloud scheme and a highly accurate semi-Lagrangian tracer transport scheme, which has been applied to the moisture, cloud water and cloud ice. The atmospheric component is coupled directly the ocean model which is based on the GFDL MOM2 code and has been specifically matched to the atmospheric model in order to avoid the added complication of a flux coupler. The ocean model is run at a resolution of 1.875° EW x 0.9375° NS with 31 levels in the vertical. The interactive land-surface scheme treats 13 land surface/vegetation types and 9 soil types and also includes a multi-layer snow cover scheme. A multi-layer thermodynamic and dynamic ice model has been developed for simulating sea ice. Additional details of the CGCM are given in Gordon et al. 2002.

The CGCM is typically integrated for the period 1871–2100. In the current project we have used CGCM output generated using the A2:m20 emissions scenario. The A2 family of emissions scenario is summarised in the IPCC Special Report on Emission Scenarios (http://www.grida.no/climate/ipcc/emission/index.htm ) as follows. “The family represents a differentiated world. Compared to the A1 storyline it is characterized by lower trade flows, relatively slow capital stock turnover, and slower technological change. The A2 world "consolidates" into a series of economic regions. Self-reliance in terms of resources and less emphasis on economic, social, and cultural interactions between regions are characteristic for this future. Economic growth is uneven and the income gap between now-industrialized and developing parts of the world does not narrow, unlike in the A1 and B1 scenario families.”

## 4.2 CCAM

The CSIRO Cubic Conformal Atmospheric Model (CCAM, McGregor 2005; McGregor and Dix 2001, 2008) has been used to downscale the CSIRO-Mk3 global climate predictions. CCAM includes a fairly comprehensive set of physical parameterizations. The GFDL parameterization for long-wave and short-wave radiation (Schwarzkopf and Fels, 1991) is employed, with interactive cloud distributions determined by the liquid and ice-water scheme of Rotstayn (1997). The model employs a stability-dependent boundary layer scheme based on Monin-Obukhov similarity theory (McGregor et al., 1993). A canopy scheme is included, as described by Kowalczyk et al. (1994), having six layers for soil temperatures, six layers for soil moisture (solving Richard's equation), and three layers for snow. The cumulus convection scheme uses mass-flux closure, as described by McGregor (2003), and includes both downdrafts and detrainment.

CCAM is formulated on a conformal-cubic grid which covers the globe, but can be stretched by utilising the Schmidt (1977) transformation to provide higher resolution in an area of interest. This is illustrated in Figure 3 where the CCAM grid configuration is shown for the current project. By periodically (6-hourly) applying a scale-selective Gaussian digital filter (Thatcher and McGregor 2008), CCAM follows the CGCM wind and surface pressure fields on the broad-scale (for length scales approximately the width of Australia). Other fields such as moisture and temperature are calculated without any form of nudging.

Because of its higher resolution, CCAM is, in principle, able to generate more accurate climate predictions over Australia, with particular emphasis on the Sydney region. CCAM was integrated for the period 1961–2100 for the purposes of the current study and meteorological boundary conditions suitable for use with TAPM–CTM were generated for the period 1996–2005, 2021–2030 and 2051–2060.

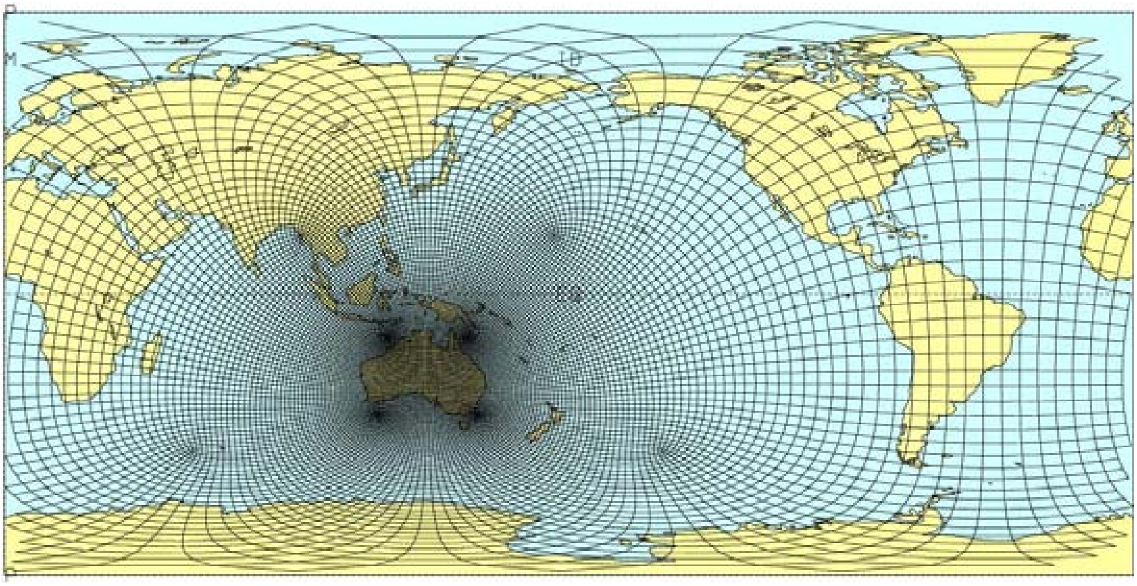

Figure 3. Conformal-cubic C48 grid used for Australian simulations. The resolution over Australia is about 60 km.

## 4.3 TAPM–CTM

TAPM–CTM is a mesoscale atmospheric modelling system with the ability to undertake numerical weather prediction and complex chemical transformation modelling. The system has three major components as briefly discussed below.

### 4.3.1 TAPM- numerical weather prediction

A nestable, three-dimensional Eulerian numerical weather and air quality prediction system, TAPM (Hurley 2005), was used for the prediction of meteorological fields including wind velocity, temperature, water vapour mixing ratio (including clouds), radiation and turbulence. The air quality component of TAPM, which includes a simple chemical transformation mechanism, was not used in the current study.

The meteorological component of TAPM is an incompressible, non-hydrostatic, primitive equation model with a planar horizontal coordinate system and a terrain-following vertical coordinate. Momentum equations are solved for the horizontal wind components and an incompressible continuity equation is solved for the vertical velocity. Scalar equations are solved for potential virtual temperature and the specific humidity of water vapour, cloud water/ice, rain and snow. The Exner pressure function is split into hydrostatic and non-hydrostatic components and a Poisson equation is optionally solved for the non-hydrostatic component. Turbulence is solved using equations of turbulence kinetic energy and eddy dissipation rate. Surface energy exchange is modelled using a big-leaf vegetation canopy scheme and a multi-layer soil scheme in which the vertical transport of heat and moisture is modelled. The surface energy model treats 39 vegetation/land use categories, including eight urban/industrial categories.

For the current study TAPM was configured with three nested grids (60 x 70 rows and columns in the horizontal and centred on Sydney) with cells spacing's of 12, 6 and 3 km (Figure 4). The model was configured with 25 levels in the vertical with levels centred on the following heights (m)- 10, 25, 50, 100, 150, 200, 250, 300, 400, 500, 600, 750, 1000, 1250, 1500, 1750, 2000, 2500, 3000, 3500, 4000, 5000, 6000, 7000, 8000.

Boundary conditions for the 12–km TAPM-CTM grid were generated by linear interpolation of 6-hourly CCAM wind, ambient temperature, specific humidity and sea surface temperature fields. The boundary conditions from the 6–km and 3–km grids were generated from corresponding 12–km and 6–km TAPM simulations and updated at 15 minute intervals. In this way, atmospheric climate change as modelled by the CGCM and downscaled by CCAM is able to force the mesoscale flows (sea breezes, katabatic and anabatic winds) which influence air quality within the Sydney basin.

### 4.3.2 CTM- chemical transport modelling

A three-dimensional Eulerian chemical transport model (CTM; Cope et al., 2004), with the capability of modelling the emission, transport, chemical transformation, wet and dry deposition of an arbitrary number of gaseous and aerosol species was used for the current project. The CTM was run as an inline module to TAPM and was called within the main time-marching loop of the host model at 300s intervals (this coupled version of TAPM and the CTM is henceforth called TAPM–CTM).

The governing equation for the CTM is the semi-empirical advection-diffusion equation for reactive species, written in a scaled form in which geometric scaling factors (map factors) are introduced into the governing equation to enable alternative coordinate systems to be treated (Toon et al. 1988). In the case of TAPM–CTM, the map factors are selected to match the TAPM coordinate system and the same horizontal grid system is also used. With each call of the CTM the instantaneous meteorological fields generated by TAPM are interpolated to the CTM grid and then used to drive the trace gas species processes of advection and diffusion, and the generation of temperature dependent emissions (see below) and chemical reaction rate coefficients.

TAPM-CTM features a generic, hybrid, stiff ordinary differential equation solver (McRae et al. 1982); is coupled to a text-driven chemical compiler, and thus can be configured to run with a range of chemical transformation schemes. The Lurmann, Carter, Coyner mechanism (LCC; Lurmann et al., 1987), with extensions to include the chemistry of methane, methanol, ethanol, methyl *tert*-butyl ether, isoprene, hydrogen peroxide and sulfur dioxide (see Table 1 and Harley et al., 1993) was used in the current study. Although newer mechanisms (e.g. Carbon Bond

2005, Yarwood et al. 2005) are now available, the LCC mechanism was used in the current study because it has previously been extensively applied to modelling photochemical smog in the GMR with good results (e.g. Cope et al. 2003) and because the Sydney emissions inventory (see below) is currently speciated for this mechanism. Moreover, a preliminary comparison of the ozone concentrations predicted by LCC and Carbon Bond 2005 undertaken for a related project (Galbally et al. 2008) did not reveal significant differences between the two mechanisms.

Table 1. Chemical species used by the LCC mechanism

| Species code | Species name | Species code | Species name |
|---|---|---|---|
| | | Differential Species[1] | |
| NO | nitric oxide | MGLY | methyl glyoxal |
| $NO_2$ | nitrogen dioxide | PAN | peroxyactyl nitrate |
| $O_3$ | ozone | $RO_2$ | total $RO_2$ radicals |
| HONO | nitrous acid | $MCO_3$ | $CH_3CO_3$ radical |
| $HNO_3$ | nitric acid | ALKN | alkyl nitrate |
| $HNO_4$ | pernitric acid | ALKA | $C_4$+ alkanes |
| $N_2O_5$ | dinitrogen pentoxide | ETHE | ethene |
| $NO_3$ | nitrogen trioxide | ALKE | $C_3$+ alkenes |
| $HO_2$ | hydroperoxy radical | TOLU | toluene |
| CO | carbon monoxide | AROM | higher aromatics |
| HCHO | formaldehyde | DIAL | unknown dicarbonyls |
| ALD2 | acetaldehyde | CRES | cresol |
| MEK | methyl ethyl ketone | NPHE | nitrophenols |
| | | Steady-State Species[2] | |
| OSD | oxygen singlet D | $RO_2N$ | alkyl nitrate $RO_2$ |
| O | atomic oxygen | $RO_2P$ | phenol $RO_2$ |
| OH | hydroxyl radical | $BZN_2$ | benzaldehyde N-$RO_2$ |
| $RO_2R$ | general $RO_2$ | BZO | phenoxy radical |
| $R_2O_2$ | general $RO_2$ | | |
| | | Added Species | |
| $H_2O_2$ | hydrogen peroxide | $NH_3$ | ammonia |
| MeOH | methanol | NIT | aerosol nitrate |
| EtOH | ethanol | $SO_2$ | sulfur dioxide |
| MTBE | methyl *tert*-butyl ether | $SO_3$ | sulfur trioxide |
| ISOP | isoprene | $CH_4$ | methane |

[1] These species are assumed to be relatively slowly reacting so their time evolution is determined by solving a rate equation.

[2] These species are assumed to reach rapid equilibrium with other species in the mechanism. As such, advective and diffusive transport is ignored and the concentration at any time is calculated from a series of algebraic equations derived from the assumption that chemical production balances chemical loss.

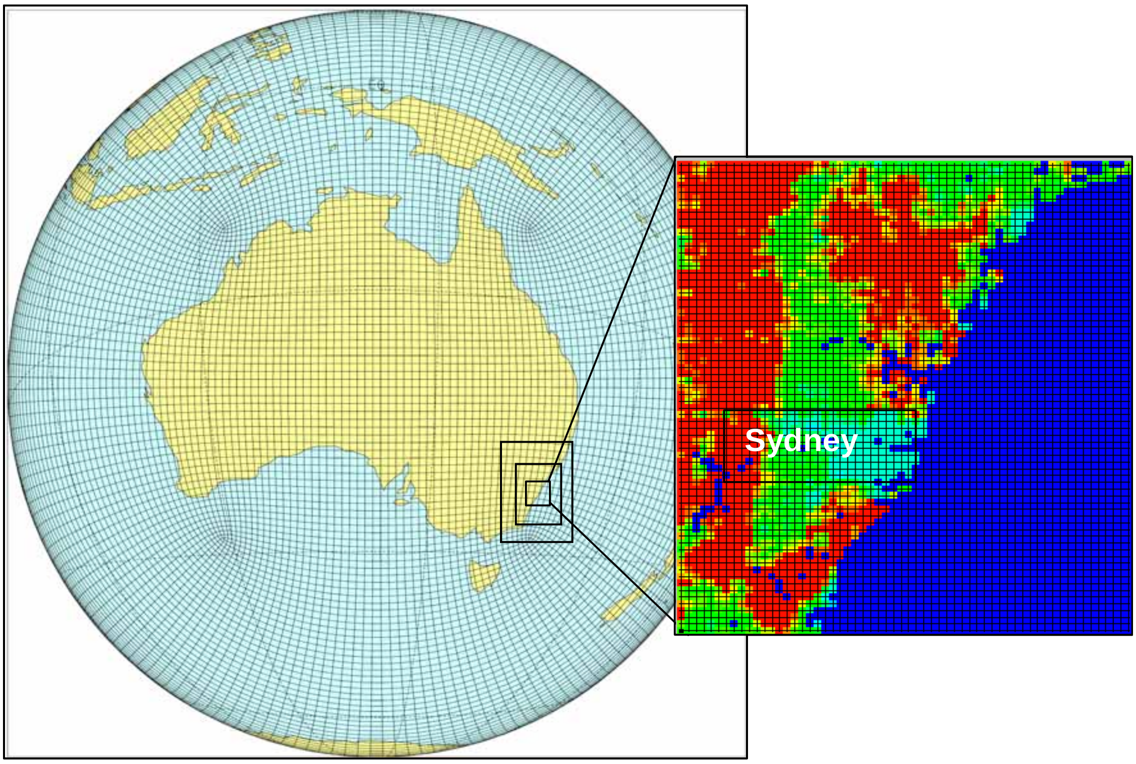

Figure 4. Schematic diagram showing the stretched computational grid of CCAM and the three uniform grids (12, 6 and 3 km cell spacing) used by TAPM–CTM.

### 4.3.3 Emissions inventory- anthropogenic and biogenic

Motor vehicle emissions for the study were based on the Sydney Greater Metropolitan Region (GMR) on-road mobile source inventory (DECC 2007). Industrial, commercial and domestic emissions were taken from the Metropolitan Air Emissions Inventory (Carnovale et al. 1996). Emissions from natural sources ($NO_x$ from bacterial activity in soils; VOC emissions from plants) were also modelled (see Azzi et al., 2005 and references therein). Table 2 shows a set of indicative summer day emission rates for various anthropogenic source groups and for the natural emissions source group.

Of particular relevance for the current project is the treatment of anthropogenic and natural emissions which vary with ambient temperature. Of the three precursor groups listed in Table 2, the VOCs are the most temperature dependent group, with natural emissions, evaporative emissions from motor vehicles and from storage and transfer (i.e. re-fuelling) known to vary significantly on an hourly and daily basis in response to the diurnal changes in ambient temperature. Non-diesel tailpipe emissions of VOC, $NO_x$ and CO are also known to vary with ambient temperature. In the current project, the temperature dependency of tailpipe emissions of all the precursor species, and the evaporative VOC emissions from motor vehicles and re-fuelling losses have been parameterised using simple bi-linear functions (Figure 5) which were originally developed for TAPM (Hurley 2005).

Table 2. Daily anthropogenic and biogenic/natural precursor emissions for the greater Sydney region

| | **$NO_x$** | | **VOC** | | **CO** | |
|---|---|---|---|---|---|---|
| | (t/day) | (%) | (t/day) | (%) | (t/day) | (%) |
| Petrol vehicle exhaust | 155 | 34 | 129 | 32 | 1712 | 65 |
| Diesel vehicle exhaust | 80 | 17 | 5 | 1 | 71 | 3 |
| Petrol vehicle evaporative | 0 | 0 | 38 | 9 | 0 | 0 |
| Commercial-domestic and surface industrial | 66 | 14 | 232 | 57 | 137 | 5 |
| Elevated industrial | 159 | 35 | 2 | 1 | 732 | 28 |
| Natural | 1–1.4 | N/A | 600 | N/A | 0 | N/A |

In the case of the tailpipe emissions, it can be seen that the emissions of VOC and CO are minimised at 25ºC and increase by 20–40% per 10ºC of temperature change away from 25ºC. $NO_x$ emissions on the other hand are a monotonic decreasing function of temperature for all temperatures in the modelled range. The evaporative emissions temperature function is essentially a bi-linear representation of the exponential Reddy vapour generation equation (Reddy 1989) and can be seen to result in a factor of two variation of the evaporative emissions as the ambient temperature increases from 25 to 35 ºC.

Table 2 also shows that the natural VOC emissions are a major source group. However, this result has to be interpreted with care because, as shown in Figure 6, the natural emission fluxes (i.e. emissions per unit area) are approximately 10 times lower than the anthropogenic VOC fluxes. However, the natural emissions are more widely distributed in space, thus leading to emission totals which are large compared to the anthropogenic total, but are a function of the summation area. Even so, the natural emissions of VOCs in particular are considered to be a significant precursor source because the emitted compounds are generally highly reactive (e.g. isoprene) and are also know to be a strong function of temperature (and radiation). Because of the important role played by natural and biogenic emissions and the rapid response of such emissions to short-term variations in temperature and radiation, these emission fluxes are calculated ‘inline’ in TAPM–CTM using a natural emissions model driven by prognostic, gridded temperature and radiation fields. A description of this model is given in Azzi et al. (2005) and references therein. As an indication of the level of detail contained in the natural emissions scheme, Figure 7 shows a schematic diagram of the 10–level vegetation canopy model which is used to model VOC emissions from trees.

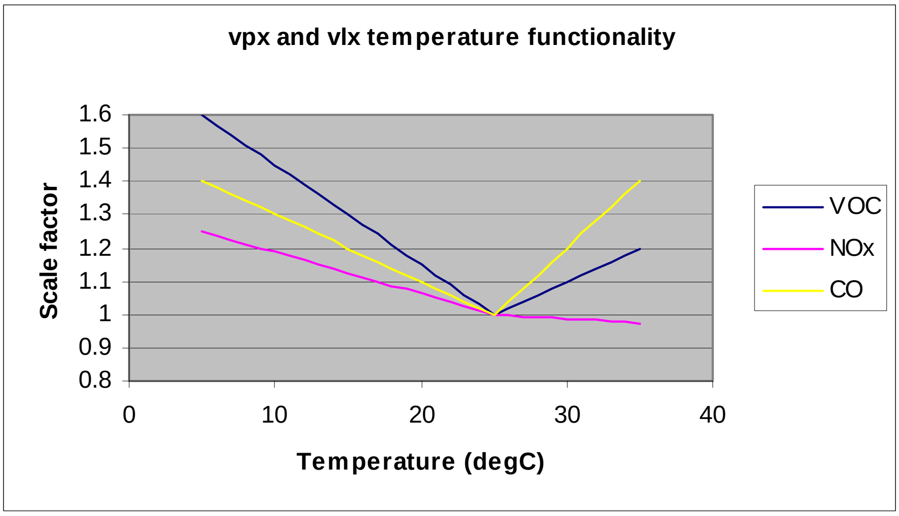

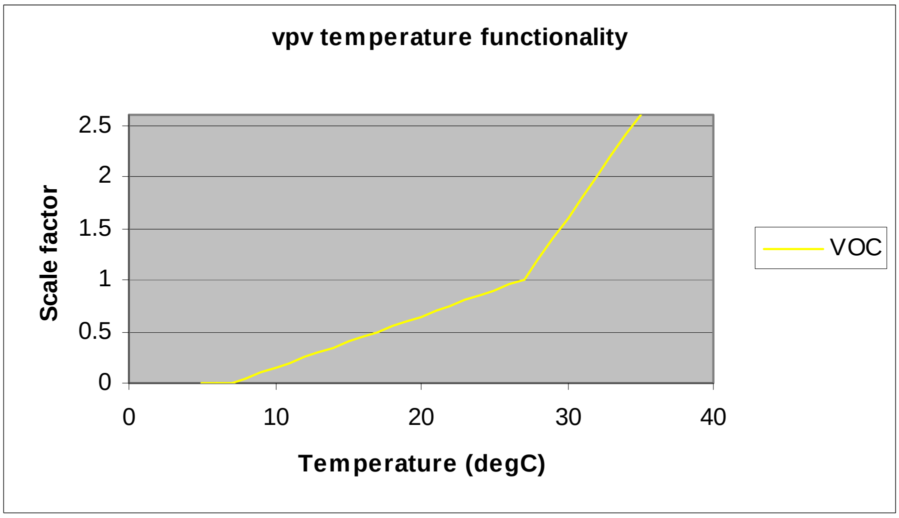

Figure 5. Top: TAPM ambient temperature scale functions for the tailpipe emissions of $NO_x$, VOC and CO (vpx = petrol-fuelled vehicle; vlx = lpg fuelled-d vehicle). Bottom: scale function for the evaporative emission of VOC from petrol fuelled motor vehicles (vpv = petrol-fuelled evaporative).

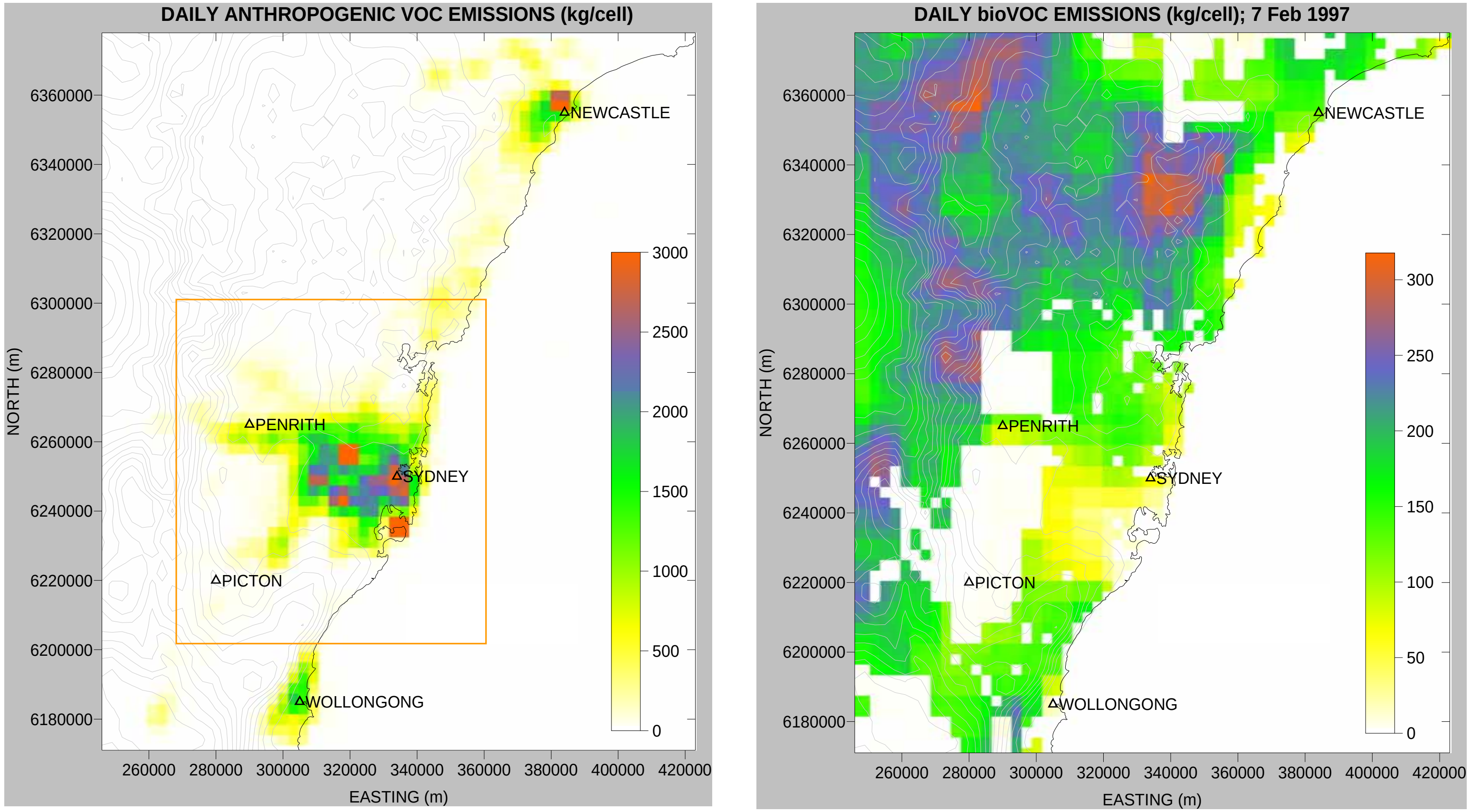

Figure 6. Left: spatial distribution of daily anthropogenic VOC emissions for the greater Sydney region. Right: spatial distribution of daily biogenic VOC emissions. The VOC emissions for both source groups have been adjusted for the diurnal temperatures observed on 7th February 1997.

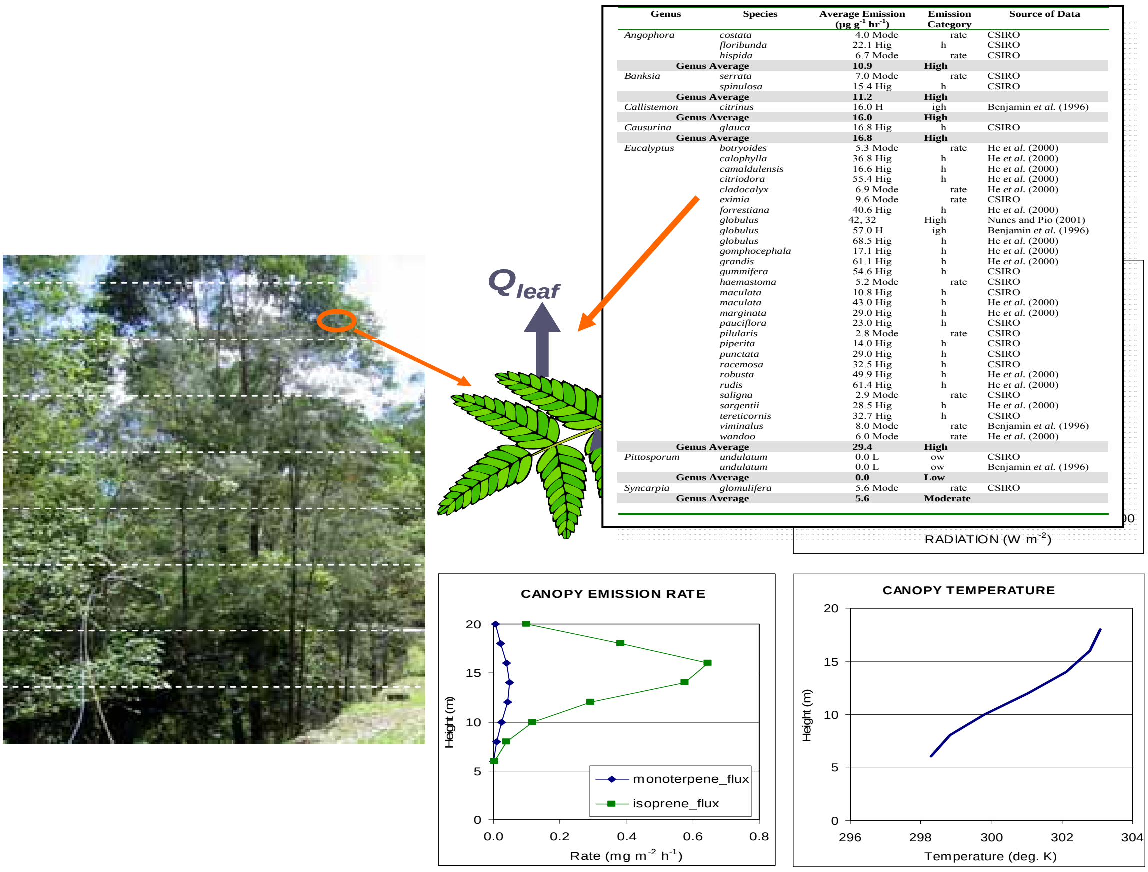

| Genus | Species | Average Emission ($\mu g\ g^{-1}\ hr^{-1}$) | Emission Category | Source of Data |
|---|---|---|---|---|
| *Angophora* | *costata* | 4.0 Mode | rate | CSIRO |
| | *floribunda* | 22.1 Hig | h | CSIRO |
| | *hispida* | 6.7 Mode | rate | CSIRO |
| **Genus Average** | | **10.9** | **High** | |
| *Banksia* | *serrata* | 7.0 Mode | rate | CSIRO |
| | *spinulosa* | 15.4 Hig | h | CSIRO |
| **Genus Average** | | **11.2** | **High** | |
| *Callistemon* | *citrinus* | 16.0 H | igh | Benjamin *et al.* (1996) |
| **Genus Average** | | **16.0** | **High** | |
| *Causurina* | *glauca* | 16.8 Hig | h | CSIRO |
| **Genus Average** | | **16.8** | **High** | |
| *Eucalyptus* | *botryoides* | 5.3 Mode | rate | He *et al.* (2000) |
| | *calophylla* | 36.8 Hig | h | He *et al.* (2000) |
| | *camaldulensis* | 16.6 Hig | h | He *et al.* (2000) |
| | *citriodora* | 55.4 Hig | h | He *et al.* (2000) |
| | *cladocalyx* | 6.9 Mode | rate | He *et al.* (2000) |
| | *eximia* | 9.6 Mode | rate | CSIRO |
| | *forrestiana* | 40.6 Hig | h | He *et al.* (2000) |
| | *globulus* | 42, 32 | High | Nunes and Pio (2001) |
| | *globulus* | 57.0 H | igh | Benjamin *et al.* (1996) |
| | *globulus* | 68.5 Hig | h | He *et al.* (2000) |
| | *gomphocephala* | 17.1 Hig | h | He *et al.* (2000) |
| | *grandis* | 61.1 Hig | h | He *et al.* (2000) |
| | *gummifera* | 54.6 Hig | h | CSIRO |
| | *haemastoma* | 5.2 Mode | rate | CSIRO |
| | *maculata* | 10.8 Hig | h | CSIRO |
| | *maculata* | 43.0 Hig | h | He *et al.* (2000) |
| | *marginata* | 29.0 Hig | h | He *et al.* (2000) |
| | *pauciflora* | 23.0 Hig | h | CSIRO |
| | *pilularis* | 2.8 Mode | rate | CSIRO |
| | *piperita* | 14.0 Hig | h | CSIRO |
| | *punctata* | 29.0 Hig | h | CSIRO |
| | *racemosa* | 32.5 Hig | h | CSIRO |
| | *robusta* | 49.9 Hig | h | He *et al.* (2000) |
| | *rudis* | 61.4 Hig | h | He *et al.* (2000) |
| | *saligna* | 2.9 Mode | rate | CSIRO |
| | *sargentii* | 28.5 Hig | h | He *et al.* (2000) |
| | *tereticornis* | 32.7 Hig | h | CSIRO |
| | *viminalus* | 8.0 Mode | rate | Benjamin *et al.* (1996) |
| | *wandoo* | 6.0 Mode | rate | He *et al.* (2000) |
| **Genus Average** | | **29.4** | **High** | |
| *Pittosporum* | *undulatum* | 0.0 L | ow | CSIRO |
| | *undulatum* | 0.0 L | ow | Benjamin *et al.* (1996) |
| **Genus Average** | | **0.0** | **Low** | |
| *Syncarpia* | *glomulifera* | 5.6 Mode | rate | CSIRO |
| **Genus Average** | | **5.6** | **Moderate** | |

Figure 7. Schematic diagram of the multi-level canopy model used to estimate biogenic VOC emissions from tree canopies. Left- the tree canopy is divided into vertical layers. Top- A look–up table generated from a Sydney–based observation programme provides normalised leaf–level emission rates. Centre- leaf-level emission rates are calculated as a function of leaf temperature ($T_{leaf}$) and photo-synthetically active radiation (PAR). Right, the in-canopy variation of radiation and temperature are described using simple parameterisations. Centre-bottom, biogenic emissions fluxes (here for monoterpenes and isoprene) are calculated for each canopy layer and summed to give a total flux.

## 5. SYSTEM PERFORMANCE

An important component of this project is an assessment of the capability of the dynamical downscaling system to reproduce the observed fields of the relevant environmental variables with a level of skill which justifies the use of the system for undertaking climate projection modelling for future decades. In the following section we will briefly consider the performance of CCAM before having a more detailed look at the capability of TAPM–CTM for generating high resolution temperature, wind, and ozone concentration fields within the Greater Sydney region. Information with respect to the performance of CGCM can be found in CSIRO (2007) and in Collier et al. (2004).